ChemComm

COMMUNICATION

View Article Online
View Journal | View Issue

Cite this: *Chem. Commun.*, 2015, 51, 13086

Received 8th March 2015,
Accepted 7th July 2015

DOI: 10.1039/c5cc01963j

www.rsc.org/chemcomm

Efficient and highly selective boron-doped carbon materials-catalyzed reduction of nitroarenes†

Yangming Lin,[ab] Shuchang Wu,[b] Wen Shi,[b] Bingsen Zhang,[b] Jia Wang,[b] Yoong Ahm Kim,[c] Morinobu Endo[d] and Dang Sheng Su*[be]

Exploring the potential catalytic applications of boron-doped carbon materials is a fascinating challenge. Here we describe that boron-doped onion-like carbon and carbon nanotubes as metal-free catalysts exhibit excellent catalytic activity and stability in nitroarene reduction under a stoichiometric amount of reductant.

Heteroatom-doped carbon materials as metal-free catalysts have attracted extensive attention over the past few years, being promising candidates in catalysis.[1] For instance, nitrogen-doped graphene or carbon nanotubes (CNTs) were shown to be excellent catalysts for aerobic oxidation of benzyl alcohol and cyclohexane.[2] Boron atoms, having a comparable atomic size and three valence electrons for binding with carbon atoms, could be incorporated into the carbon matrix, leading to the formation of p-type (or hole) doped carbon materials with desired electronic structures.[3] However, apart from the oxygen reduction reaction,[4] these boron-doped catalysts have been rarely reported for other catalytic reactions. It is therefore interesting to explore the potential catalytic applications of such doped carbon materials.

Aromatic amines are important intermediates and key precursors in the synthesis of various fine chemicals and pharmaceuticals.[5] Traditionally, nitro group reductions are carried out using various transition metal or precious metal catalysts.[6] Recently, a series of great achievements have been made in the presence of metal-free materials using excess hydrazine hydrate (4–8 equiv.) as a reductant. For example, Ma and co-workers reported that reduced graphene oxide exhibited excellent catalytic performance for hydrogenation of nitrobenzene.[7] Su *et al.* developed a class of hydrogen peroxide-oxidized CNTs and demonstrated their validity for nitroarene reduction.[8] Arai *et al.* studied chemoselective transfer hydrogenation of nitrobenzene over oxygen- and nitrogen-doped activated carbon.[9] Nevertheless, the undesired decomposition of hydrazine hydrate and intermediate hydrogen waste products have been responsible for its low utilization efficiency. The development of a high utilization efficiency of hydrazine hydrate still remains a demanding task.

In this work, boron-doped onion-like carbon (B-OLC) or CNTs (B-CNTs) were obtained *via* a high-temperature annealing of nanodiamond or acid-treated CNTs in a graphite furnace using boron acid as boron precursor, respectively. We report for the first time that the obtained boron-doped carbon materials can be used as efficient catalysts for nitroarene hydrogenation and the utilization efficiency of hydrazine hydrate is close to 80% under certain conditions. For comparison, pristine OLC and CNTs samples were tested for the same reaction.

The HRTEM images in Fig. S1A–C (ESI†) show the structures of pristine OLC and doped OLC consisting of multilayer sp^2 fullerene-like shells. The identified interlayer spacing of about 0.340 nm in the shell of OLC corresponds to the (002) of turbostratic graphite carbons. In general, boron doping into graphite structure leads to a slight decrease in interlayer spacing d_{002} compared to that of the host starting graphite, depending upon the amount of doped boron atoms.[10] Interestingly, in the present case of B-OLC-2, d_{002} increases slightly presumably because of the onion-like morphology being kept after boron doping into the hexagonal lattice. When increasing the content of boron, the ordering of the fullerene-like structure of B-OLC-3 may be disrupted and thus leads to the slight decrease of the interlayer spacing (Fig. S1C, ESI†). There are no distinctive differences in the diameter and morphology of CNTs and B-CNTs (Fig. S1D–F, ESI†).

XPS and Raman spectroscopy were employed to study the physicochemical properties of these samples. Fig. S2A and

[a] *School of Chemistry and Materials Science, University of Science and Technology of China, Hefei, 230001, P. R. China*
[b] *Shenyang National Laboratory for Materials Science, Institute of Metal Research, Chinese Academy of Sciences, 72 Wenhua Road, Shenyang 110016, P. R. China. E-mail: dssu@imr.ac.cn*
[c] *School of Polymer Science and Engineering, Chonnam National University, 77 Yongbong-ro, Buk-gu Kwangju, 500-757, Republic of Korea*
[d] *Carbon Institute of Science and Technology, Shinshu University, 4-17-1 Wakasato, Nagano, 380-8553, Japan*
[e] *Department of Inorganic Chemistry, Fritz Haber Institute of the Max Planck Society, Faradayweg 4-6, Berlin, 14195, Germany*

† Electronic supplementary information (ESI) available: Materials preparation, characterization methods and additional figures. See DOI: 10.1039/c5cc01963j

2B (ESI†) show that the spectra of B-OLC and B-CNTs could be deconvoluted into six components: boron atom cluster (B1, ~186.5 eV), B_4C (B2, ~187.6 eV), substitutional boron species BC_3 (B3, ~188.8 eV), BC_2O (B4, that is B–C=C–O, ~190.1 eV), B-N (B5, ~191.1 eV, originating from the chemical bonding between inherent trace nitrogen species and boron source after annealing) and B_2O_3-related (B6, >192.0 eV).[11] The total concentrations of boron species on B-OLC are about 1.5–5.0 at%. On the contrary, with an increasing amount of boron precursor (increases from 8 wt% to 25 wt%), the as-prepared B-CNTs samples did not exhibit an obvious increase in the content of boron (0.8–1.2 at%, Fig. S2B, ESI†). This may be ascribed to the well-ordered surface structure of CNTs. The detailed results are displayed in Fig. S2C and D. In addition, the value of I_D/I_G increases from 1.9 of OLC to 2.5 of B-OLC-2, revealing that the introduction of boron produces much more structural defects. The weakened 2D peak and upshift of the G peak for B-OLC-2 indicate that boron has been successfully doped into the sp^2 carbon framework and further influences the electronic structure of fullerene-like layers (Fig. S3A, ESI†).[1c] A similar result could be observed in pristine CNTs and B-CNTs-2 (Fig. S3B, ESI†).

As shown in the energy-filtered transmission electron microscopy (EFTEM) images of the representative B-OLC-2 and B-CNTs samples, boron atoms are homogenously distributed in the carbon framework (see Fig. 1B, C, E and F).

Table 1 displays the catalytic behaviors of various carbon materials for nitrobenzene reduction to aniline under different conditions. In the absence of any catalyst, only 17.8% of nitrobenzene conversion after 4 h at 100 °C is found (Table 1, entry 1). When 4 equiv. hydrazine hydrate are added into the reaction, all doped carbon materials exhibit an enhanced catalytic performance compared to pristine ones (Table 1, entries 2–9), even higher than the best metal-free catalysts and some metal-based catalysts reported in the literature.[7,12] The highest yield rates for aniline over B-OLC-2 and B-CNTs-2 reach 593 and 1360 μmol m^{-2} h^{-1}, respectively. B-OLC-3 leads to a lower selectivity for aniline which may be attributed to the fact that a high content of boron can lead to the formation of disordered fullerene-like layer structure and a decrease of surface area (Table 1, entry 5). There are no obvious differences in the selectivity for aniline over various B-CNTs catalysts (Table 1, entries 7–9) because of the similar content of boron species. Notably, as a stoichiometric amount of hydrazine hydrate (1.5 equiv.) is introduced, B-OLC-2 and B-CNTs-2 catalysts still possess excellent catalytic activity, and the conversion of nitrobenzene and selectivity for aniline exceed 80% and 97% (Table 1, entries 12 and 15), respectively. In this case, the utilization efficiency of hydrazine hydrate in nitrobenzene reduction is close to 80% within 4 h. These results reveal the crucial role of boron for nitrobenzene reduction. When CNTs without acid-treatment serve as a starting material, the obtained B-CNTs-2-P sample does not exhibit a better catalytic performance than B-CNTs-2, implying that the metal impurity may not play a key role in improving the catalytic performance (Table 1, entries 15 and 16).

Table 1 Catalytic activity of different carbon materials for nitrobenzene reduction[a]

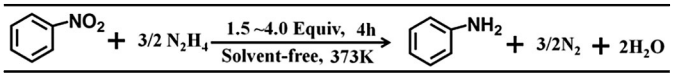

Entry	Catalyst	S_{BET} (m^2 g^{-1})	N_2H_4 (equiv.)	Con. (%)	Sel. (%)	R^b (μmol m^{-2} h^{-1})
1	—	—	4	17.8	96.2	—
2	OLC	463	4	32.1	98.5	170
3	B-OLC-1	431	4	>99	80.3	461
4	B-OLC-2	400	4	>99	95.3	593
5	B-OLC-3	363	4	>99	83.1	567
6	CNTs	214	4	29.9	89.5	313
7	B-CNTs-1	188	4	>99	93.3	1228
8	B-CNTs-2	179	4	>99	98.3	1360
9	B-CNTs-3	175	4	>99	92.9	1313
10	—	—	1.5	4.8	95.6	—
11	OLC	463	1.5	9.1	98.2	60
12	B-OLC-2	400	1.5	80.2	97.3	482
13	CNTs	214	1.5	12.1	90.5	127
14	CNTs-P	226	1.5	13.1	92.5	134
15	B-CNTs-2	179	1.5	81.8	98.1	1127
16	B-CNTs-2-P	192	1.5	80.9	98.9	1041

[a] Reaction conditions: 10 mg catalyst, 10 mmol (1.23 g) substrate. [b] Yield rate of aniline per m^2 of catalyst surface.

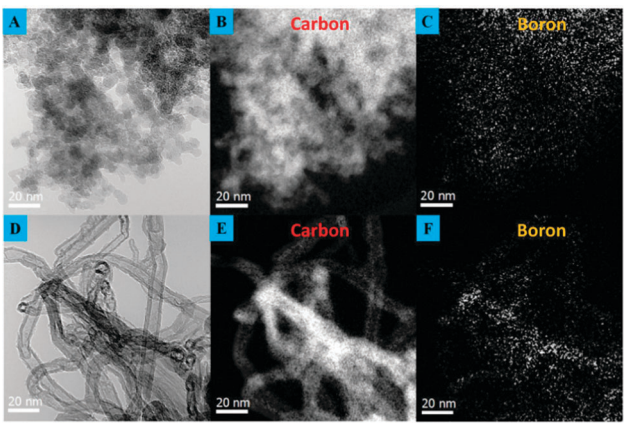

Fig. 1 (A) and (D) TEM images of B-OLC-2 and B-CNTs-2 samples. EFTEM images of carbon and boron of (B) and (C) B-OLC-2 and (E) and (F) B-CNTs-2 samples.

Through simple centrifugation, we could achieve the separation of doped carbon materials from the reaction solution and reuse them for the next reaction. Fig. 2A and B illustrate that doped catalysts exhibit good stability for the tested ten successive runs. Moreover, Raman results indicate that no obvious change could be observed between fresh and used doped carbon materials, verifying the structural stability of these catalysts (Fig. S4, ESI†).

In order to study the general applicability of the boron-doped carbon materials-catalyzed reduction reactions, nineteen kinds of nitroarenes were tested under the optimized reaction conditions. The results in Table 2 indicate that good conversions (>99%) for all the substrates and selectivities (>88%) for the desired products could be obtained. These findings demonstrate that the doped carbon materials possess excellent chemoselective reduction ability for structurally diverse and functional nitro compounds with C=C, C=N, C≡N, OH, ether, halogen and ester groups.

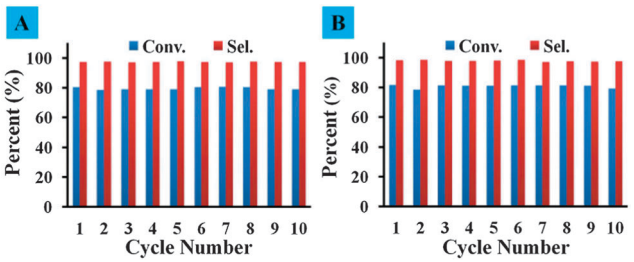

Fig. 2 Recycling test of (A) B-OLC-2 and (B) B-CNTs-2 in nitrobenzene reduction. Reaction conditions: 10 mg catalyst, 10 mmol (1.23 g) substrate, 1.5 equiv. N_2H_4, 100 °C, 4 h.

In our previous studies, carbonyl group (C═O, ~531.5 eV) on the surface of oxidized CNTs instead of metal impurity was considered to play an important role in nitrobenzene reduction.[8,13] However, as shown in Fig. S5 (ESI†), the oxygen species of pristine OLC and CNTs are mainly attributed to surface-adsorbed C–O or C–OH groups (~532.8 eV), indicating that the weak activity of both pristine OLC and pristine CNTs may be derived from structural defects and edges.[7] Moreover, we also do not find the signal of C═O bond in O 1s spectra of the B-OLC-2 and B-CNTs-2 catalysts (Fig. 3A). The deconvoluted O 1s spectra of these samples are ascribed to the characterization peaks (surface C–O–B, B═O and B–O) of B_2O_3. It seems that the B_2O_3 species instead of oxygen species plays a positive role in improving the catalytic performance in nitrobenzene reduction. As described earlier, six kinds of boron species involving boron atom clusters, B_4C, substitutional boron species BC_3, BC_2O (B–C═C–O), BN and B_2O_3 were observed in boron-doped carbon materials (Fig. 1A). In order to determine which boron species of doped catalysts was the active one, various commercial model catalysts were further investigated. Fig. 3B illustrates that none of the other commercial catalysts (B, B_4C, BN and B_2O_3) exhibit the enhanced catalytic performance, revealing that the substitutional boron species BC_3 may play a determining role in nitrobenzene reduction. This result is also supported by the control experiment of normalized specific surface area of various catalysts (Table S1, ESI†). Incorporating boron into a carbon network would tune the electronic structure of graphite-like layers and form different charged sites on the surface of carbon materials.[14] Owing to the larger electronegativity of carbon with respect to boron, boron (electron-deficient) in the lattice is a positively charged site.[4a,15] Moreover, it was reported that boron-doped carbon materials exhibited excellent ability for hydrogen storage because of the weak chemisorptions between boron and hydrogen.[16] In this case, N_2H_4 (a strong electron-donating reagent) may be adsorbed on the site of lattice boron forming a weak B–H bond (meanwhile, hydrogen is activated), and thus stabilizing the hydrogen intermediate products and avoiding the fast loss of hydrogen as H_2. When nitroarene substrates get close enough to the benzene ring of the catalyst through π–π interactions, the oxygen atoms of nitro group would abstract the activated hydrogen atoms,[17] and finally leading to the high selectivity for desired products and achieving the efficient utilization of N_2H_4. A detailed mechanism exploration is ongoing in our group.

Table 2 Catalytic activity of B-OLC-2 and B-CNTs-2 for various nitroarenes[a]

Entry	Catalyst	Substrate	Product	Con. (%)	Sel. (%)
1[b]	B-OLC-2	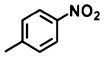	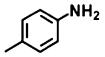	>99	96.5
	B-CNTs-2			>99	97.3
2[b]	B-OLC-2	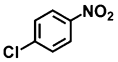	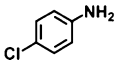	>99	94.5
	B-CNTs-2			>99	96.3
3[c]	B-OLC-2			>99	93.0
	B-CNTs-2			>99	94.9
4[d]	B-OLC-2	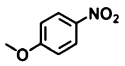	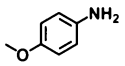	>99	96.2
	B-CNTs-2			>99	97.1
5[e]	B-OLC-2	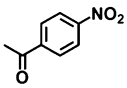	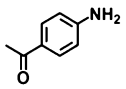	>99	96.8
	B-CNTs-2			>99	97.4
6	B-OLC-2	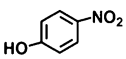	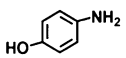	>99	95.4
	B-CNTs-2			>99	93.9
7	B-OLC-2	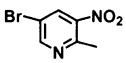	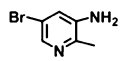	>99	93.2
	B-CNTs-2			>99	92.9
8	B-OLC-2	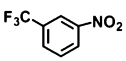	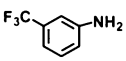	>99	94.2
	B-CNTs-2			>99	93.1
9[f]	B-OLC-2	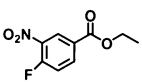	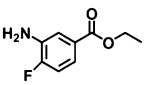	>99	89.2
	B-CNTs-2			>99	90.3
10[f]	B-OLC-2	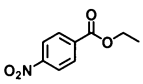	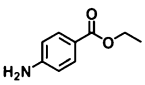	>99	91.4
	B-CNTs-2			>99	90.9
11	B-OLC-2	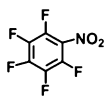	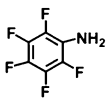	>99	91.9
	B-CNTs-2			>99	90.2
12[g]	B-OLC-2	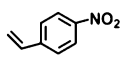	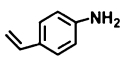	>99	88.4
	B-CNTs-2			>99	90.9
13[h]	B-OLC-2	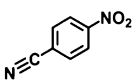	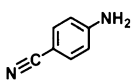	>99	92.2
	B-CNTs-2			>99	91.2
14	B-OLC-2	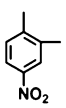	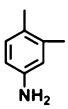	>99	96.9
	B-CNTs-2			>99	97.1
15[i]	B-OLC-2	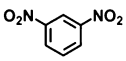	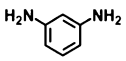	>99	96.7
	B-CNTs-2			>99	97.1
16[h]	B-OLC-2	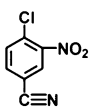	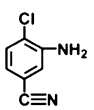	>99	90.2
	B-CNTs-2			>99	90.6
17[i]	B-OLC-2			>99	96.1
	B-CNTs-2			>99	95.3

Table 2 (*continued*)

Entry	Catalyst	Substrate	Product	Con. (%)	Sel. (%)
18[i]	B-OLC-2	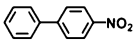	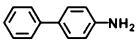	>99	97.9
	B-CNTs-2			>99	98.0
19[i]	B-OLC-2	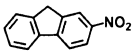	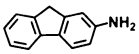	>99	97.2
	B-CNTs-2			>99	97.0

[a] Reaction conditions: 10 mg catalyst, 1 mmol substrate, 4 equiv. N_2H_4, 100 °C, 4 h. [b] 50 mg catalyst, 5 mmol substrate, 1.5 equiv. N_2H_4, ethanol as solvent, 70 °C, 4 h. [c] 20 mg catalyst, 5 mmol substrate, 1.5 equiv. N_2H_4, 100 °C, 5 h. [d] 100 mg catalyst, 5 mmol substrate, 1.5 equiv. N_2H_4, ethanol as solvent, 70 °C, 4 h. [e] 40 mg catalyst, 2 mmol substrate, 1.5 equiv. N_2H_4, ethanol as solvent, 80 °C, 4 h. [f] 10 mg catalyst, 0.5 mmol substrate, 1.5 equiv. N_2H_4, THF as solvent, 80 °C, 4 h. [g] 10 mg catalyst, 0.5 mmol substrate, 1.5 equiv. N_2H_4, ethanol as solvent, 70 °C, 8 h. [h] 10 mg catalyst, 0.5 mmol substrate, 4 equiv. N_2H_4, ethanol as solvent, 80 °C, 10 h. [i] 10 mg catalyst, 1 mmol substrate, 4 equiv. N_2H_4, ethanol as solvent, 100 °C, 8 h.

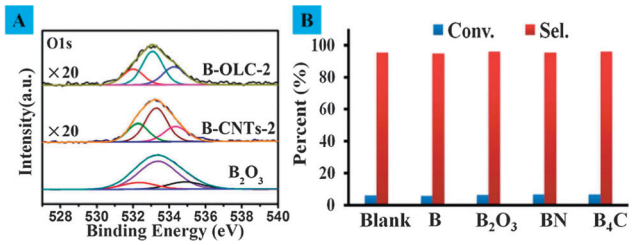

Fig. 3 (A) XPS O 1s spectra of B-OLC-2, B-CNTs-2 and B_2O_3. (B) Catalytic activity of various commercial model catalysts for nitrobenzene reduction. Reaction conditions: 40 mg catalyst, 10 mmol (1.23 g) nitrobenzene, 1.5 equiv. N_2H_4, 100 °C, 4 h.

In conclusion, two kinds of boron-doped carbon materials (onion-like carbon and carbon nanotubes) are found to be excellent catalysts in the hydrogenation of nitroarene reduction. The results show that substitutional boron species BC_3 may play an important role in improving the catalytic performance and efficient utilization of N_2H_4. We believe that this work will open up a new route for the applications of boron-doped carbon materials in reduction reactions.

The authors thank Dr Linhui Yu and Rui Huang for their kind help in this study. This work was supported by the National Natural Science Foundation of China (21133010, 51221264, 21261160487), MOST (2011CBA00504), and the "Strategic Priority Research Program" of the Chinese Academy of Sciences (grant no. XDA09030103).

Notes and references

1 (*a*) D. S. Su, S. Perathoner and G. Centi, *Chem. Rev.*, 2013, **113**, 5782; (*b*) Y. Lin and D. Su, *ACS Nano*, 2014, **8**, 7823; (*c*) Y. Lin, X. Pan, W. Qi, B. Zhang and D. S. Su, *J. Mater. Chem. A*, 2014, **2**, 12475.
2 (*a*) J. Long, X. Xie, J. Xu, Q. Gu, L. Chen and X. Wang, *ACS Catal.*, 2012, **2**, 6223; (*b*) Y. Cao, H. Yu, J. Tan, F. Peng, H. Wang, J. Li, W. Zheng and N. B. Wong, *Carbon*, 2013, **57**, 433.
3 T. B. Martins, R. H. Miwa, A. J. R. da Silva and A. Fazzio, *Phys. Rev. Lett.*, 2007, **98**, 196803.
4 (*a*) L. Yang, S. Jiang, Y. Zhao, L. Zhu, S. Chen, X. Wang, Q. Wu, J. Ma, Y. Ma and Z. Hu, *Angew. Chem.*, 2011, **31**, 7270; (*b*) Z. H. Sheng, H. L. Gao, W. J. Bao, F. B. Wang and X. H. Xia, *J. Mater. Chem.*, 2012, **22**, 390; (*c*) E. Pourazadi, E. Haque, W. Zhang, H. T. Harris and A. I. Minett, *Chem. Commun.*, 2013, **49**, 11068; (*d*) G. Jo and S. Shanmugam, *Electrochem. Commun.*, 2012, **25**, 101.
5 (*a*) R. S. Downing, P. J. Kunkeler and H. van Bekkum, *Catal. Today*, 1997, **37**, 121; (*b*) G. Wegener, M. Brandt, L. Duda, J. Hofmann, B. Klesczewski, D. Koch, R. Kumpf, H. Orzesek, H. Pirkl, C. Six, C. Steinlein and M. Weisbeck, *Appl. Catal., A*, 2001, **221**, 303.
6 (*a*) K. Junge, B. Wendt, N. Shaikh and M. Beller, *Chem. Commun.*, 2009, 1769; (*b*) S. Srinivasan and X. Huang, *Chirality*, 2008, **20**, 265; (*c*) R. G. de Noronha, C. C. Romao and A. C. Fernandes, *J. Org. Chem.*, 2009, **74**, 6960; (*d*) L. H. Gong, Y. Y. Cai, X. H. Li, Y. N. Zhang, J. Su and J. S. Chen, *Green Chem.*, 2014, **16**, 3746; (*e*) Y. N. Zhang, X. H. Li, Y. Y. Cai, L. H. Gong, K. X. Wang and J. S. Chen, *RSC Adv.*, 2014, **4**, 60873; (*f*) X. H. Li, X. C. Wang and M. Antonietti, *Chem. Sci.*, 2012, **3**, 2170; (*g*) X. H. Li, Y. Y. Cai, L. H. Gong, W. Fu, K. X. Wang, H. L. Bao, X. Wei and J. S. Chen, *Chem. – Eur. J.*, 2014, **20**, 16732; (*h*) A. Corma and P. Serna, *Science*, 2006, **313**, 332; (*i*) R. V. Jagadeesh, A. E. Surkus, H. Junge, M. M. Pohl, J. Radnik, J. Rabeah, H. Huan, V. Schünemann, A. Brückner and M. Beller, *Science*, 2013, **342**, 1073; (*j*) M. Takasaki, Y. Motoyama, K. Higashi, S. H. Yoon, I. Mochida and H. Nagashima, *Org. Lett.*, 2008, **10**, 1601; (*k*) D. Cantillo, M. Baghbanzadeh and C. O. Kappe, *Angew. Chem., Int. Ed.*, 2012, **51**, 10190; (*l*) H. U. Blaser, H. Steiner and M. Studer, *ChemCatChem*, 2009, **1**, 210; (*m*) K. Layek, M. L. Kantam, M. Shirai, D. Nishio-Hamane, T. Sasaki and H. Maheswaran, *Green Chem.*, 2012, **14**, 3164; (*n*) Y. Chen, J. Qiu, X. Wang and J. Xiu, *J. Catal.*, 2006, **242**, 227; (*o*) A. Corma, P. Concepción and P. Serna, *Angew. Chem., Int. Ed.*, 2007, **46**, 7266.
7 Y. Cao, D. Ma, C. Wang, J. Guan and X. Bao, *Chem. Commun.*, 2011, **47**, 2432.
8 S. Wu, G. Weng, R. Schlögl and D. S. Su, *Phys. Chem. Chem. Phys.*, 2015, **17**, 1567.
9 S. I. Fujita, H. Watanabe, A. Katagiri, H. Yoshida and M. Arai, *J. Mol. Catal. A: Chem.*, 2014, **393**, 257.
10 (*a*) C. E. Lowell, *J. Am. Ceram. Soc.*, 1967, **50**, 142; (*b*) M. Endo, C. Kim, T. Karaki, T. Tamaki, Y. Nishimura, M. J. Matthews, S. D. M. Brown and M. S. Dresselhaus, *Phys. Rev. B: Condens. Matter Mater. Phys.*, 1998, **58**, 8991.
11 (*a*) T. Shirasaki, A. Derré, M. Ménétrier, A. Tressaud and S. Flandrois, *Carbon*, 2000, **38**, 1461; (*b*) S. Jacques, A. Guette, X. Bourrat, F. Langlais, C. Guimon and C. Labrugere, *Carbon*, 1996, **34**, 1135.
12 (*a*) R. V. Jagadeesh, G. Wienhöfer, F. A. Westerhaus, A. E. Surkus, M. M. Pohl, H. Junge, K. Junge and M. Beller, *Chem. Commun.*, 2011, **47**, 10972; (*b*) Z. Zhao, H. Yang, Y. Li and X. Guo, *Green Chem.*, 2014, **16**, 1274.
13 (*a*) S. Wu, G. Weng, J. Wang, J. Rong, B. Zong and D. S. Su, *Catal. Sci. Technol.*, 2014, **4**, 4183; (*b*) S. Wu, G. Weng, B. Zhong, B. Zhang, X. Gu, N. Wang and D. S. Su, *Chin. J. Catal.*, 2014, **35**, 914.
14 B. Li and D. S. Su, *J. Phys. Chem. C*, 2013, **117**, 17485.
15 (*a*) L. Ferrighi, M. Datteo and C. D. Valentin, *J. Phys. Chem. C*, 2014, **118**, 223; (*b*) C. H. Choi, S. H. Park and S. Woo, *ACS Nano*, 2012, **6**, 7084; (*c*) M. Grujicic, G. Cao, A. M. Rao, T. M. Tritt and S. Nayak, *Appl. Surf. Sci.*, 2003, **214**, 289.
16 (*a*) L. Firlej, S. Roszak, B. Kuchta, P. Pfeifer and C. Wexler, *J. Chem. Phys.*, 2009, **131**, 164702; (*b*) M. Sankaran and B. Viswanathan, *Carbon*, 2007, **45**, 1628.
17 S. Wu, G. Weng, X. Liu, B. Zhong and D. S. Su, *ChemCatChem*, 2014, **6**, 1558.